

See discussions, stats, and author profiles for this publication at: <https://www.researchgate.net/publication/260245236>

Two-Step Adsorption of Endogenous Asphaltenic Surfactants at the Bitumen–Water Interface

ARTICLE *in* ENERGY & FUELS · OCTOBER 2012

Impact Factor: 2.79 · DOI: 10.1021/ef300186e

CITATIONS

6

READS

21

4 AUTHORS, INCLUDING:



Mathieu Neuville

EcoZimut

11 PUBLICATIONS 11 CITATIONS

SEE PROFILE



Alain Cagna

Teclis Sarl France

26 PUBLICATIONS 839 CITATIONS

SEE PROFILE



Sanchez Michael

2 PUBLICATIONS 6 CITATIONS

SEE PROFILE

Two-Step Adsorption of Endogenous Asphaltenic Surfactants at the Bitumen–Water Interface

Mathieu Neuville,^{*,†} Francis Rondelez,[†] Alain Cagna,[‡] and Michael Sanchez[‡]

[†]Total SA, CRES, BP 22, 69360 Solaize, France

[‡]IT Concepts-Teclis, 69770 Longesaigne, France

ABSTRACT: We have performed hanging droplet measurements of a straight-run bitumen (SRB) and its corresponding deasphalted oil (DAO) to investigate the adsorption process at the bitumen–water interface (pH 2.7, $T = 90\text{ }^{\circ}\text{C}$). The analysis of the time and surface pressure dependences of the viscoelastic properties show that two types of endogenous surfactants (called A and B) compete for the same interface in the case of SRB. The A species adsorb first, and their molecular characteristics (size and bulk concentration) can be obtained by fitting the data with a diffusion-limited adsorption model. They form fluid-like interfacial layers. The B species, that diffuse more slowly toward the interface, eventually replace the A species to form highly viscous and hardly compressible interfacial layers. The B species belong to the asphaltene solubility class because they are removed by the *n*-heptane fractionation. They are not present in DAO, which only contains the A species. We surmise that those are also asphaltenes but of higher aliphaticity and/or lower state of aggregation. The possibility that they are resins cannot, however, be eliminated at this stage.

INTRODUCTION

Asphaltenes are a key constituent of bitumen and control important bulk properties, such as their viscosity, elasticity, etc. They are known to be composed of polycyclic (aromatic and naphthenic) molecules with aliphatic side chains and doped with some metals and polar heteroatoms (such as nitrogen, oxygen, and sulfur). Therefore, it comes as no surprise that they can be surface-active. Numerous studies in the literature show that small amounts of asphaltenes added to organic liquids can lower the liquid–water or liquid–air interfacial tension quite significantly.^{1–4} In a previous work,⁵ we have shown that asphaltenes are also active at the bitumen–water interface. The experiments were performed at $90\text{ }^{\circ}\text{C}$ on seven different straight-run bitumen in contact with an aqueous phase at pH 2.7. At this temperature, the bitumen viscosity is in a medium range and the adsorption process was slow enough to be conveniently monitored. The acidic pH value ensured that the acidic groups naturally present in bitumen were protonated and electrostatic interactions, salt effects, or further solubilization in the aqueous phase could be neglected. The time dependence of the interfacial tension was described quantitatively by a diffusion-limited adsorption model, yielding molecular sizes for the endogenous surfactants, consistent with asphaltenes in a non-aggregated, monomeric, form.⁶ Their bulk concentrations were found to be much lower than the total asphaltenes measured by the saturates, aromatics, resins, and asphaltenes (SARA) method. They were in the range from 2×10^{-4} to 2×10^{-3} g/g, in agreement with recent results by Czarnecki et al.^{7,8}

In this paper, we report comparative experiments between one straight-run bitumen (later called SRB) and its parent C_7 -deasphalted oil (later called DAO). The surface dilational elastic modulus and viscosity are measured in addition to the static interfacial tension, providing a characterization of the interfacial layer more complete than in our previous work. Moreover, the adsorption process is monitored during a time

period that is 10 times longer. We will show that these new data reveal the presence of at least two different types of surfactants in the straight-run bitumen, opening the possibility of competitive exchanges at the bitumen–water interface, a previously unsuspected feature in the formation of the adsorbed layer.

MATERIALS AND METHODS

Samples. A straight-run Eastern Europe bitumen (SRB) was used for the experiments. Its parent deasphalted oil (DAO) was prepared by precipitation of SRB in a 40:1 solution of *n*-heptane stirred at room temperature for 12 h. The precipitated fraction was filtered, and the remaining solution was treated in a rotary evaporator to remove the solvent and obtain a DAO containing mostly maltenes. Their SARA compositions and elemental analysis were determined using the NFT 60-115 standard method and atomic absorption spectroscopy, respectively. The results are given in Tables 1 and 2. The density

Table 1. SARA Analysis (wt %) of the SRB and DAO Samples

SARA composition (wt %)	saturates	aromatics	resins	asphaltenes
SRB	6.7	56	27.9	9.4
DAO	10	75.3	14.4	0.3

and viscosity of the samples at $90\text{ }^{\circ}\text{C}$ were obtained using an oscillating capillary densitometer and a Brookfield viscosimeter, respectively. The applied shear rate in the viscosity measurements was 150 s^{-1} to avoid shear-thinning effects. The results are shown in Table 3.

Experimental Methods. Static Measurements. The value of the interfacial tension, γ , was measured using the same hanging drop apparatus as in our previous study.⁵ The droplet volume was varied

Received: March 6, 2012

Revised: October 16, 2012

Published: October 16, 2012

Table 2. Atomic Composition (wt %) of the SRB and DAO Samples

atomic composition (wt %)	C	H	N	S	O	Ni (ppm)	V (ppm)
SRB	85.3	10.3	0.7	2.9	<1	67	230
DAO	85.1	11.1	0.51	2.7	<1	19	68

Table 3. Bulk Viscosity and Density (Measured at 90 °C) of the SRB and DAO Samples

data taken at 90 °C	viscosity, η (Ns m ⁻²)	density (kg m ⁻³)
SRB	2.13	964
DAO	0.32	915

between 10 and 300 μL , but 100 μL was the most common value. The curvature radius at the apex was typically 3–5 mm. The optical analysis of the drop profile was performed to an accuracy of 1 μm . The diameter of the capillary used to suspend the droplet was 1 mm. The cell was pressurized with air at a few bars to prevent adsorption of the gas bubbles produced by degassing onto the drop surface. This effect is especially present in DAO because of its low viscosity and would perturb the determination of the interfacial tension because the drop shape is then distorted. The experiments were repeated on three different samples rather than 3 times on a single sample to minimize aging and degradation upon heating. The accuracy on the interfacial tension determination by this static method was of the order of 0.1 mN m⁻¹, and the repeatability of the measurements was found to be ± 1.5 mN m⁻¹.

Dynamic Measurements. The drop tensiometer was also used in the dynamic mode by submitting the volume of the suspended droplet to periodic variations. Recording simultaneously the interfacial tension $\gamma(t)$, surface area $A(t)$, and drop volume $V(t)$ during this compression–expansion process yields the dilational viscoelastic modulus E of the bitumen–water interface.

$$E = \frac{d\gamma}{dA/A} = \frac{d\gamma}{d \ln(A)}$$

For sinusoidal oscillations, the changes in $A(t)$ and $\gamma(t)$ are out of phase by an angle θ ; therefore, E is a complex quantity, $E = E' + iE''$, with real and imaginary components defined as

$$E' = |E| \cos(\theta)$$

$$E'' = |E| \sin(\theta)$$

$$|E| = \sqrt{E'^2 + E''^2}$$

E' is the dilational elastic modulus (or storage modulus) that measures the energy stored during a periodic deformation of the interface and has dimensions of mN m⁻¹. E'' is the dilational viscous modulus (or loss modulus) that accounts for energy dissipation in the interfacial layer. We will call ν the surface dilational viscosity, with $\nu = E''/\omega$ ($\omega = 2\pi f$, with f being the oscillation frequency). It has dimensions of mN m⁻¹ s.

In these experiments, the maximum amplitude of the volume oscillation, ΔV , was 10 μL , corresponding to 10% of the initial volume. A frequency of 0.02 Hz was selected empirically as a good compromise to satisfy two opposite criteria. On one hand, it should be low enough to minimize the influence of the bulk viscous stresses that could lead to non-physical observations.⁹ On the other hand, it should be high enough to ensure that the composition of the interface layer does not change significantly during the time of measurement. These compositional changes could be due to either increased adsorption during the time of the measurement or molecular exchanges between the interface and the bulk reservoir by diffusional relaxation during the compression–expansion cycle.¹⁰

We are confident that the first criterion was met at the selected frequency because the interfacial tension was found to be time-

independent when measured immediately after the drop formation (that is to say, when the interface is still free of adsorbed surfactants). It would have followed the oscillations otherwise.¹¹ Moreover, the measured value was the same as in the absence of oscillations. We will discuss the second criterion in detail in the Discussion. In short, we believe that it was fulfilled for the adsorption of the B-type molecules in SRB based on optical observations of contracted suspended droplets and for the adsorption of A-type molecules for SRB and DAO but only at small surface pressures based on the surface viscosity data.

The mechanical oscillations were generally maintained for four cycles (corresponding to 200 s). This fixes the minimum time interval separating two measurements by the dynamic method, keeping in mind that the adsorption process extends over several thousands of seconds.

The accuracy on E' and $E'' = \nu/\omega$ was of the order of 0.2 mN m⁻¹, and the repeatability of the measurements was found to be ± 3 mN m⁻¹.

RESULTS

The evolution with time of the interfacial tension, γ , surface dilational elastic modulus, E' , and surface dilational viscosity, ν , are shown in Figures 1–3, respectively. The origin of time has

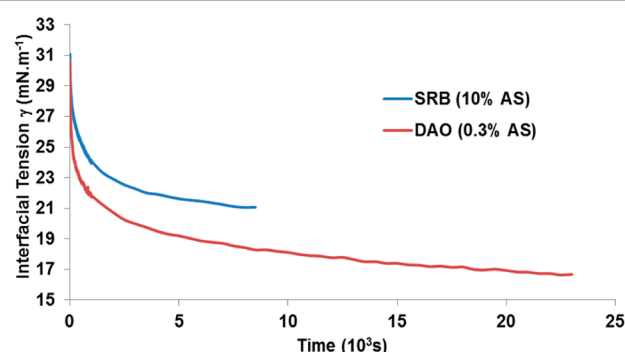


Figure 1. Time evolution of the interfacial tension, γ , at the SRB (or DAO)–acidified water interface. $T = 90$ °C, and pH 2.7. The asphaltene content is 10% (by weight) for SRB and 0.3% for DAO.

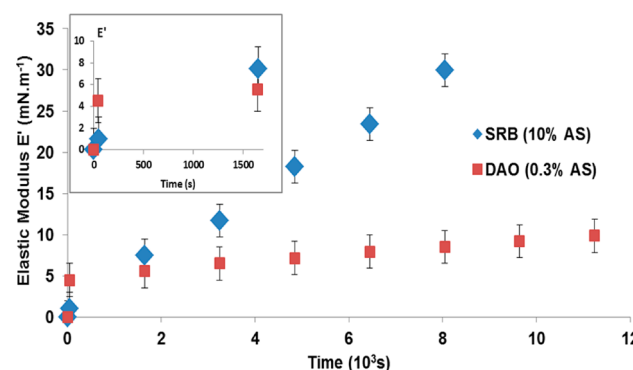


Figure 2. Time evolution of the surface dilational elastic modulus, E' , for the SRB (or DAO)–acidified water interface. $T = 90$ °C, and pH 2.7. The inset shows an enlargement of the data points at times shorter than 2000 s.

been taken 5 s after the formation of the droplet at the tip of the needle to account for mechanical equilibration. In Figure 1, one observes a large decrease of γ in both SRB and DAO, indicating the progressive adsorption on the interface of surface-active constituents contained in the bulk of the drop. The maximum time range is 23 000 s for these experiments. Figure 2 shows that E' increases steadily up to a value of 30.0

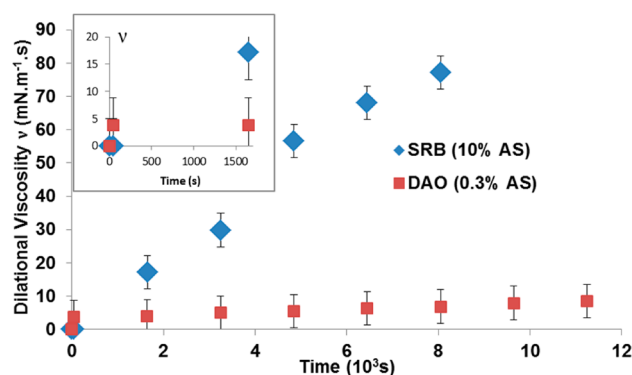


Figure 3. Time evolution of the surface dilational viscosity, ν , for the SRB (or DAO)–acidified water interface. Other conditions are the same as in Figure 2.

mN m^{-1} for SRB at 8000 s. For DAO, it starts to level off at 6 mN m^{-1} after only a few hundred seconds and then increases slowly up to a low value of 8.5 mN m^{-1} after 8500 s. The E' data at three specific times (0, 100, and 8000 s) are given in Table 4. Figure 3 shows similar behavior for ν , with maximum

Table 4. Values of the Surface Dilational Elastic Modulus, E' , Measured at Three Different Times during the Adsorption Process

surface dilational elastic modulus, E' , of the bitumen–water interface (mN m^{-1})			
	$t = 0 \text{ s}$	$t = 100 \text{ s}$	$t = 8000 \text{ s}$
SRB	0	1.0	30.0
DAO	0	4.5	8.5

values of 6.9 and $77.1 \text{ mN m}^{-1} \text{ s}$ for DAO and SRB, respectively. The ν data at 0, 100, and 8000 s are given in Table 5. One remarks that, at 100 s, the elasticity and viscosity for

Table 5. Values of the Surface Dilational Viscosity, ν , at Three Different Times during the Adsorption Process

surface dilational viscosity, ν , of the bitumen–water interface ($\text{mN m}^{-1} \text{ s}$)			
	$t = 0 \text{ s}$	$t = 100 \text{ s}$	$t = 8000 \text{ s}$
SRB	0	0	77.1
DAO	0	3.8	6.9

DAO are much larger than those for SRB. This is due to the smaller bulk viscosity of DAO. The surfactants diffuse more rapidly in the bulk and accumulate faster at the interface than in SRB. This short-time behavior is outlined in the insets of Figures 2 and 3. The opposite behavior is observed at long times, where the measured elasticity and viscosity values are much larger for SRB than for DAO. At 8000 s, for instance, the ratio is 5.5:1 for E' and 9.1:1 for ν .

To verify that the interfacial tension is controlled by the Brownian diffusion of surface-active molecular species coming from the bulk, we have replotted the interfacial tension data of Figure 1 by dividing the experimental time values by the bulk viscosities, η_{SRB} and η_{DAO} , given in Table 3. With this rescaling, the variations for DAO and SRB become close over the whole time range, as shown in Figure 4. On the basis of the quasi-superposition of the two curves (the remaining difference is well within experimental repeatability), it would be tempting to claim that the two interfacial layers are formed with the same

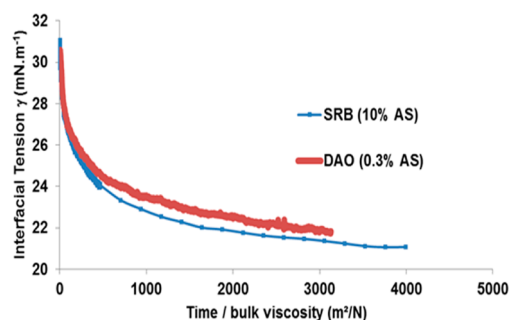


Figure 4. Interfacial tension, γ , for the SRB (or DAO)–acidified water interface as a function of time divided by the bulk viscosity.

molecules over the whole time range. The rescaled surface elastic modulus and surface viscosity curves, however, do not support this last statement. From looking at Figures 5 and 6, it

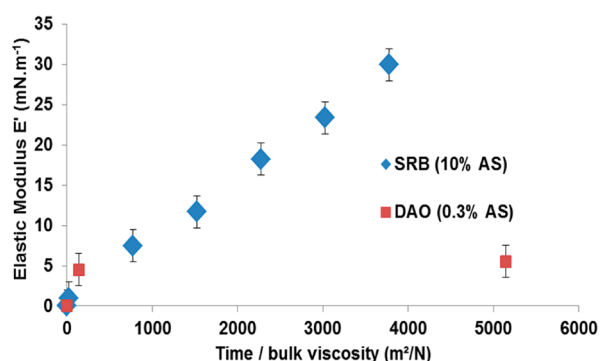


Figure 5. Surface dilational elastic modulus, E' , for the SRB (or DAO)–acidified water interface as a function of time divided by the bulk viscosity.

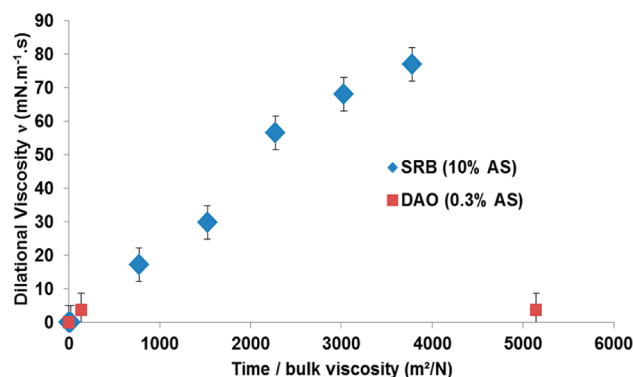


Figure 6. Time evolution of the surface dilational viscosity, ν , for the SRB (or DAO)–acidified water interface as a function of time divided by the bulk viscosity.

is evident that the E' and ν values for SRB and DAO are only similar at small times (below 1000 s) but differ considerably afterward. This point will be crucial for the interpretation of our data.

DISCUSSION

For DAO, the E' and ν values are always small, which is typical of a fluid interface. For SRB on the contrary, their strong increases at long time suggest a transition from a fluid to a viscous, hardly compressible, layer. This is corroborated by macroscopic optical observations of $200 \mu\text{L}$ suspended droplets

in contact with water for 10^4 s and whose volume is then reduced 40% by mechanical suction. As shown by the images of Figure 7, the DAO droplet keeps a regular Laplacian shape,

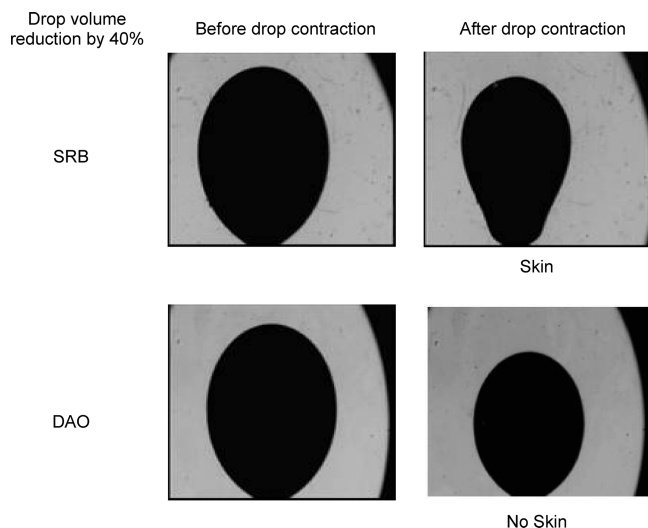


Figure 7. Projected images of 200 μL of SRB and DAO droplets (in black) in contact with acidified water (white background). The drops have been left to stabilize for 10^4 s before being submitted to a 40% volume reduction by suction.

while the SRB droplet takes an irregular, pear-like shape characteristic of an interfacial rigid film driven above its elastic limit. Similar macroscopic “skins” have already been reported at oil–water interfaces in the case of solutions containing large amounts of asphaltenes.^{12–14}

To compare in more details the SRB and DAO behaviors, we have plotted in Figure 8 the surface elastic modulus, E' , versus

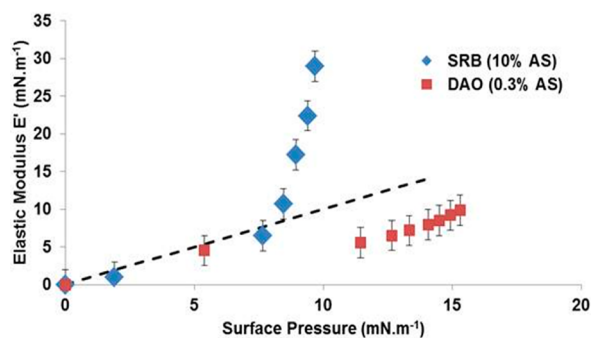


Figure 8. Surface elastic modulus, E' , versus surface pressure $\Pi = \gamma_0 - \gamma$ for the SRB (or DAO)–acidified water interface.

the surface pressure, $\Pi = \gamma_0 - \gamma$ (γ_0 is the value at $t = 0$ s). The interest of this method, proposed by Lucassen-Reynders and co-workers,¹⁵ has been demonstrated by them on several soluble monolayer systems.^{10,16} According to their studies, (i) there is always initial proportionality between E' and Π , and the slope is characteristic of the surfactant type; (ii) this representation provides an image of the equation of state of the monolayer when diffusional interexchange with bulk solution is negligible; and (iii) the measuring frequency of the dynamic hanging drop method has to be large enough to avoid temporary desorption of the adsorbed molecules into the bulk phase during the compression–expansion cycles.

At low Π , corresponding to short adsorption times, we observe, on the one hand, that E' versus Π follows a straight line of slope unity (indicated by the dotted line in Figure 8) in both SRB and DAO and up to Π values of the order of 8 mN m^{-1} . On the other hand, Figure 9 shows that ν versus Π stays

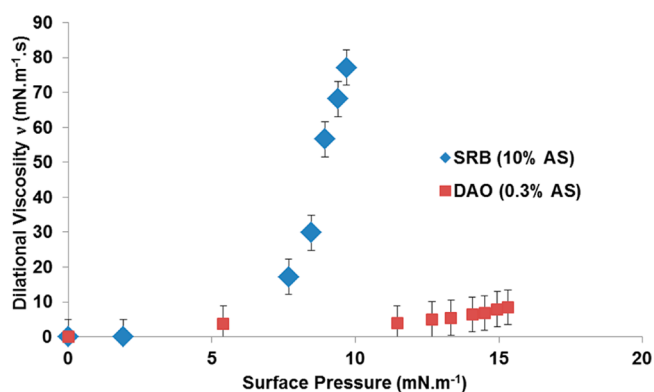


Figure 9. Surface dilational viscosity, ν , versus surface pressure $\Pi = \gamma_0 - \gamma$ for the SRB (or DAO)–acidified water interface.

close to the baseline within experimental accuracy in both samples. The similarity of the SRB and DAO surface elasticity and dilational viscosity values over this surface pressure range suggests that the two interfaces are composed of the same surface-active molecules. In the following, we will call them the A-type surfactants. These interfacial layers are elastic and fluid-like. Because the measured viscosities always stay immeasurably small, we can assume the absence of diffusional relaxation over the 50 s oscillation period. If this was not the case, such a phenomenon would have given a contribution to the measured viscosity. The interfacial layers can therefore be considered as insoluble in the time frame of our dynamic experiments. Of course, they must be regarded as soluble over the longer time scales involved in the static interfacial tension measurements.

At large pressures, corresponding to long adsorption times, the situation is totally different between DAO and SRB. In the first case, the E' data points are all situated below the proportionality line, whereas in the second case, there is a hefty increase in the pressure dependence for Π values higher than 8 mN m^{-1} . Striking differences are also observed between the two sets of dilational viscosities, ν . As shown in Figure 9, measured viscosities increase moderately in DAO and dramatically in SRB, again around a Π value of 8 mN m^{-1} . To explain that difference of behavior after an adsorption time of 1400 ± 200 s (see Figure 1 for the correspondence between the surface pressure and adsorption time), we postulate that the A-type molecules present initially in the monolayer are gradually replaced by another type of molecule. In the following, we will call them the B type. The interfacial layer in SRB at large surface pressures is little compressible and very viscous.

As suggested by one of the referees, the fact that the E' curve in DAO goes below the proportionality line indicates that diffusional relaxation is present at high surface pressures. A fraction of the adsorbed surfactants leaves the interface during the time that the monolayer is mechanically compressed. In all rigor, the elastic surface modulus is no longer equal to the Gibbs modulus and the measured surface dilational viscosity now includes a contribution of the bulk viscosity.¹⁰

Such a complication is not present in SRB. We have checked this point by performing a static compression up to the largest possible surface pressure of 14 mN m^{-1} , just before the droplet would start to crumple irreversibly. We then stop the compression and monitor the surface pressure evolution. No relaxation of the pressure value is observed over times as long as several hours. Therefore, the monolayer can certainly be considered as irreversible during the 50 s time scale used in our drop oscillating experiments. Another proof is that the measured surface viscosity is roughly 20 times higher in SRB than in DAO at the highest pressure of 9.7 mN m^{-1} (see Figure 9). If the viscosity was due in part to diffusional relaxation as in DAO, the two sets of data should scale at most according to the bulk viscosities, i.e., by a factor of 7.

Bouriat et al.¹⁷ have performed similar hanging drop measurements on asphaltene solutions deposited at the cyclohexane–water interface and for various solute concentrations. By covering an extended range of frequencies (with the help of a time–temperature superposition principle) and times, they were able to show that the adsorbed asphaltenes self-aggregate and form a structured network at large surface concentrations, with viscoelastic properties akin to a two-dimensional gel near its gelation point. For a 50 s oscillation period, their measured elastic coefficient and surface dilational elasticity for a surface pressure of 7 mN m^{-1} are comparable to our values.

Quantitative Description of the Adsorption of the A-Type Molecules in SRB and DAO. We have already discussed in a previous paper⁵ how the size, r , of the adsorbed molecules, their translational diffusion coefficient, D_T , and their bulk concentration, C_b , can be obtained by fitting the time dependence of the interfacial tension $\gamma(t)$ to a diffusion-limited, reversible adsorption process. Fainerman et al.¹⁸ have proposed equations valid for an interface that is either essentially free (at short times, ST) or already crowded (at long times, LT)

$$\Delta\gamma(t)_{\text{ST}} = \gamma_0 - \gamma(t) = -2RTC_b\sqrt{D_T\frac{t}{\pi}}$$

$$\Delta\gamma(t)_{\text{LT}} = \gamma(t) - \gamma_\infty = RT(\Gamma_{\text{sat}})^2\sqrt{\frac{\pi}{4D_Tt}}C_b^{-1}$$

where γ_0 and γ_∞ are the values taken by $\gamma(t)$ at time zero and infinite (infinite meaning that the interface has been saturated with the surface-active molecules), respectively. Γ_{sat} is the surface excess at saturation. $D_T = kT/6\pi\eta r$, where η is the bulk viscosity, T is the temperature in Kelvin, and k the Boltzmann constant.

The product of the slopes of $\Delta\gamma(t)_{\text{ST}}$ versus $t^{1/2}$ and $\Delta\gamma(t')_{\text{LT}}$ versus $(t')^{-1/2}$ yields Γ_{sat} directly.

$$\text{slope of } \Delta\gamma(t)_{\text{LT}} \times \text{slope of } \Delta\gamma(t')_{\text{ST}} = (RT\Gamma_{\text{sat}})^2$$

If one then considers that, at saturation, the bitumen–water interface is covered by close-packed disks of size r , one can calculate r from the Γ_{sat} value

$$r = (\pi N\Gamma_{\text{sat}})^{-1/2}$$

where N is the Avogadro number. Once r (or D_T) is known, C_b is obtained from the equation

$$C_b = \text{slope of } \Delta\gamma(t)_{\text{ST}} / (2RT(D_T/\pi)^{1/2})$$

The values for the slopes of $\Delta\gamma(t)_{\text{ST}}$ and $\Delta\gamma(t')_{\text{LT}}$ for SRB and DAO at pressures less than 8 mN m^{-1} (corresponding to the A

species adsorption in both samples) have been obtained by least-squares fitting the interfacial tension data of Figure 1 to straight lines, taking γ_0 and γ_∞ as the adjustable parameters. The procedure has already been described in detail in our previous paper,⁵ and the curves are not shown here. The short- and long-time domains deduced from the fit are listed in Table 6. The Γ_{sat} , D_T , r , and C_b values are given in Table 7, together with γ_0 and γ_∞ . They provide the molecular characteristics of the A-type surfactants present in DAO and SRB.

Table 6. Time Ranges (Seconds) Selected for the Adsorption of the A-Type Molecules at the SRB (or DAO)–Acidified Water Interface^a

time ranges (seconds) for the data analysis of the adsorption of the A-type surfactants		
	short-time domain (free interface) (s)	long-time domain (crowded interface) (s)
SRB	0–40	400–900
DAO	0–5	80–300

^aThe short-time regime describes the adsorption onto an interface essentially free of surface-active molecules. The long-time regime describes the adsorption onto a cluttered interface.

Nature of the A-Type Molecules in SRB and DAO. The data of Table 7 confirm our earlier statement that the interfacial layers formed during the first 900 s for SRB and 300 s for DAO are composed of the same surface-active molecules. They have identical molecular sizes (0.5 nm), produce the same amplitude of interfacial tension decrease (10 mN m^{-1}), and form interfacial layers of similarly small dilational elastic moduli and surface viscosity. From the good agreement between the experimental data at low pressures and the simple diffusion-limited model used for the fit, it can also be inferred that their adsorption is reversible.

The bulk concentration of the A-type species is found to be very low in both samples, of the order of $2 \times 10^{-1} \text{ mol m}^{-3}$.¹⁹ Assuming a molecular weight of 1000 Da, this corresponds to $2 \times 10^{-4} \text{ g/g}$, which is an extremely small fraction of the bitumen. Because the surface/volume ratio of our droplets is small, it is nevertheless amply sufficient to cover the interface with a dense monolayer.

Because they are present in DAO, the A-type species belong to a solubility class resisting *n*-heptane precipitation. They are most likely asphaltenes at the low end of the molecular-weight distribution and/or with a significant degree of aliphaticity. The possibility that they could be aromatic resins can however not be excluded.²⁰

Nature of the B-Type Molecules Specifically Present in SRB. As said before, the properties of the SRB interfacial layer changes drastically after 1400 s. We interpret this transition from a fluid to a viscous, hardly compressible monolayer as a result of the adsorption of a novel type of endogenous surfactants, different from the A type, and called the B type. The formation of the adsorbed layer thus proceeds in two steps: species A adsorb first but are gradually replaced by species B over the course of time.

There are two possible mechanisms to explain this competitive displacement by the B species: (i) their ability to induce a lower interfacial tension and (ii) a higher stability at the interface. The first argument can be dismissed because the γ values for SRB and DAO at long times are practically identical. The stability argument is more pertinent and is well-

Table 7. Quantitative Characterization of the A-Type Molecule Endogenous Surfactants^a

molecular characteristics of the A-type surfactants							
samples ($T = 90\text{ }^{\circ}\text{C}$, pH 2.7)	surface coverage ($\pm 20\%$) Γ_{sat} ($\times 10^{-6}$, mol m^{-2})	molecular size ($\pm 10\%$) r (nm)	diffusion coefficient ($\pm 10\%$) D_T ($\times 10^{-13}$, $\text{m}^2 \text{ s}^{-1}$)	concentration in bulk ($\pm 35\%$) C_b ($\times 10^{-1}$, mol m^{-3})	interfacial tension at time $t = 0$ s (free interface) γ_0 (mN m^{-1})	interfacial tension at long times (crowded interface) γ_{∞} (mN m^{-1})	interfacial tension variation $\Delta\gamma = \gamma_0 - \gamma_{\infty}$ (mN m^{-1})
SRB (10% AS)	2.1	0.5	2.5	2.5	31.5	21.1	10.4
DAO (0.3% AS)	1.8	0.5	15.5	1.8	31.5	21.2	10.3

^a D_T , C_b , and r are their translational diffusion coefficient, bulk concentration, and molecular size, respectively. Γ_{sat} is the surface excess at saturation. γ_0 is the interfacial tension extrapolated at time zero, and γ_{∞} is the interfacial tension extrapolated at infinite time. $\Delta\gamma = \gamma_0 - \gamma_{\infty}$ is the global variation of the interfacial tension because of the adsorption of the A-type molecules.

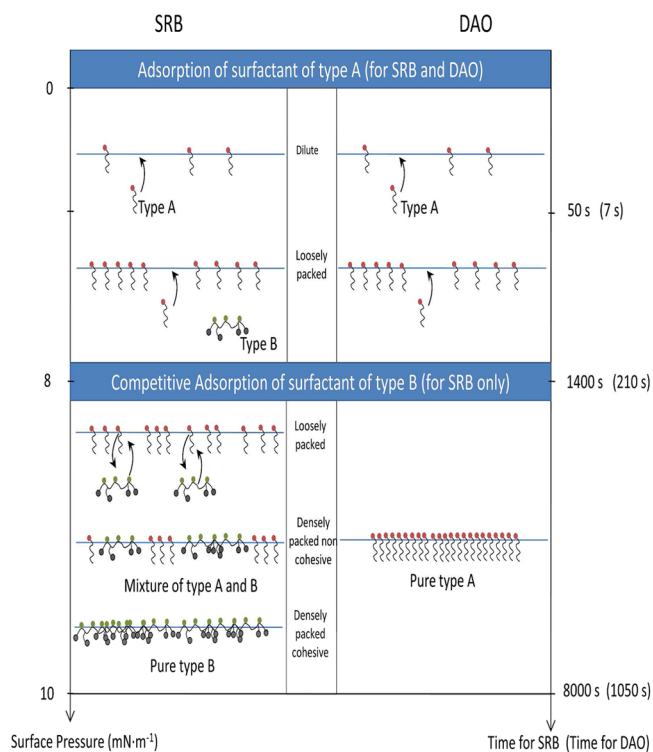
documented in polymer solutions containing a mixture of short and long chains and exposed to a solid surface.^{21,22} The short chains adsorb first because they diffuse faster as a result of their low molecular weight, but the long chains displace them in the long run because they contain a larger number of attachment points to the surface.

Because kinetic barriers to adsorption have to be considered in this second adsorption step, the Fainerman equations are not applicable and the B-type molecular characteristics cannot be determined as before. What we know for sure is that they belong to the high-molecular-weight end and aromatic fraction of the asphaltene class because they are not soluble in *n*-heptane. We also know from the data of Table 2 that they possess higher amounts of heteroatoms than the A type, in a 3.5:1 ratio for nickel and vanadium. These polar atoms or chemical groups are responsible for the strong, irreversible, molecular adsorption. They also favor intermolecular association and bonding in the plane of the interface, because of charge separations and dipolar interactions. The formation of nanoaggregates or clusters of nanoaggregates as a result of these interactions and the van der Waals attraction between their large aromatic ring systems have been amply discussed in the recent literature.^{23,24} In dilute (less than 0.1 mg/mL) solutions of a good solvent, such as toluene, individual nanoaggregates have typical sizes of 1–2 nm in linear dimension. Their growth, however, is limited by the repulsive steric hindrance of the alkyl side chains attached to the ring system, and they contain no more than 5–10 molecules. They start to associate in large clusters above a critical nanoaggregate concentration of 1–5 mg/mL.⁶ The smallest units detected in crude oils and toluene by small-angle X-ray scattering,²⁵ small-angle neutron scattering,²⁵ and also nuclear magnetic resonance (NMR)²⁶ have a size of 3–10 nm. Admitting for the moment that there is no kinetic barrier for the B-type species in our experiments (which is certainly incorrect and leads to overestimation of the size of the diffusing species), a time scale of 1400 s corresponds to a molecular size of 17 nm, which is in the same bulk part as the above value.

The consequences of asphaltene nanoaggregates on the properties of Langmuir monolayers at the air–water interface have been studied by Lobato et al.²⁷ and Orbulescu et al.²⁸ As the monolayer density is gradually increased, an interconnected net of nanoaggregates is formed. The interfacial film becomes very rigid and can even crack upon lateral mechanical compression.²⁸ Our results are in line with these observations.

Summary of the Mechanisms of Adsorption in DAO and SRB. The different mechanisms of adsorption at the SRB (or DAO)–acidified water interface are summarized in Table 8 as a function of time and surface pressure. For clarity of

Table 8. Summary of the Adsorption Mechanisms at the SRB (DAO)–Acidified Water Interface



presentation, the left (surface pressure) and right (time) ordinate axes are not drawn to scale. The red dots indicate the polar groups for the A-type molecules. The black dots indicate the polar groups for the B-type molecules, also capable of forming intermolecular bonds. The two time scales reflect the difference in bulk viscosities between DAO (values in parentheses) and SRB. In DAO, the adsorption of A-type molecules continues until the interfacial layer is fully saturated. In SRB, the adsorption occurs in two steps: the interface is first covered with A-type molecules, but they are gradually replaced by B-type molecules at times longer than 1400 s.

CONCLUSION

By performing comparative experiments on a SRB and its DAO obtained by *n*-heptane precipitation, we have shown that the adsorption process of endogenous surfactants at the bitumen–water interface is more complex than usually thought. Our measurements reveal the existence of two different surface-active species (called A and B types) in the case of SRB. Their competition for the bitumen–water interface leads to

sequential adsorption. Adsorption of the A-type molecules occurs first but is followed by a molecular exchange between the A and B types afterward. In the case of DAO, the B-type molecules are not present and the interfacial layer is formed exclusively with A-type molecules.

The A-type surfactants belong to the *n*-heptane solubility class and are either asphaltene of low molecular weight and/or high aliphaticity or resins. They form a fluid, elastic interfacial layer. The B-type surfactants belong to the class of asphaltenes that are insoluble in *n*-heptane. They are most likely present in bulk bitumen in the form of aggregates and form viscous, hardly compressible surface layers with a high dilational elastic modulus.

It is interesting to note that dynamic surface tension and dilational surface rheology measurements have been essential to detect the A-type to B-type molecular exchange in SRB. This emphasizes their importance to fully characterize bitumen–water interfaces.

AUTHOR INFORMATION

Corresponding Author

*E-mail: mathieu.neuville@total.com.

Notes

The authors declare no competing financial interest.

ACKNOWLEDGMENTS

We thank the Direction Scientifique and the Direction “Marketing Bitumes” of Total SA for their continuous interest and support of this work. We also thank the analytic department at CReS for their expert contribution in characterizing our samples.

REFERENCES

- (1) Czarnecki, J. Stabilization of water in crude oil emulsions. Part 2. *Energy Fuels* **2009**, *23*, 1253–1257.
- (2) Horváth-Szabó, G.; et al. Adsorption isotherms of associating asphaltenes at oil/water interfaces based on the dependence of interfacial tension on solvent activity. *J. Colloid Interface Sci.* **2005**, *283*, 5–17.
- (3) Poteau, S.; et al. Influence of pH on stability and dynamic properties of asphaltenes and other amphiphilic molecules at the oil/water interface. *Energy Fuels* **2005**, *19*, 1337–1341.
- (4) Sheu, E. Y.; Storm, D. A.; Shields, M. B. Adsorption kinetics of asphaltenes at toluene/acid solution interfaces. *Fuel* **1995**, *74*, 1475–1479.
- (5) Chaverot, P.; et al. Interfacial tension of bitumen–water interfaces. Part 1: Influence of endogenous surfactants at acidic pH. *Energy Fuels* **2008**, *22*, 790–798.
- (6) Mullins, O. C. The modified Yen model. *Energy Fuels* **2010**, *24*, 2179–2207.
- (7) Czarnecki, J.; Moran, K. On the stabilization mechanism of water-in-oil emulsions in petroleum systems. *Energy Fuels* **2005**, *19*, 2074–2079.
- (8) Czarnecki, J.; Tchoukov, P.; Dabros, T. Possible role of asphaltenes in stabilization of water in crude oil emulsions. *Proceedings of the 11th Annual International Conference on Petroleum Phase Behavior and Fouling*; Newark, NJ, 2010; p O24.
- (9) Freer, E. M.; Wong, H.; Radke, C. J. Oscillating drop/bubble tensiometry: Effect of viscous forces on the measurement of interfacial tension. *J. Colloid Interface Sci.* **2005**, *282*, 128–132.
- (10) Lucassen-Reynders, E. H.; Cagna, A.; Lucassen, J. Gibbs elasticity, surface dilational modulus and diffusional relaxation in nonionic surfactant monolayers. *Colloids Surf., A* **2001**, *186*, 63–72.
- (11) In their paper, Freer et al.⁹ suggest that the frequency should be adjusted in such a way that the capillary number, $Ca = \Delta\eta\omega\Delta V/\gamma a^2$, where $\Delta\eta = \eta_{\text{bulk}} - \eta_{\text{water}}$, ΔV is the amplitude of the volume oscillation, γ is the interfacial tension, and a is the droplet radius at its apex, should stay smaller than a threshold value of 2×10^{-3} . In our experimental conditions ($f = 0.02$ Hz), the capillary number was 1.7×10^{-3} for DAO and 2.8×10^{-2} for SRB. A frequency of 3.5×10^{-3} Hz would have been necessary in that later case; however, it is impractical if one wants to monitor the adsorption process. Moreover, we had no evidence of the influence of bulk viscous stresses. We plan to perform further experiments to address this question.
- (12) Gao, S.; et al. Role of bitumen components in stabilizing water-in-diluted oil emulsions. *Energy Fuels* **2009**, *23*, 2606–2612.
- (13) Jeribi, M.; et al. Adsorption kinetics of asphaltenes at liquid interfaces. *J. Colloid Interface Sci.* **2002**, *256*, 268–272.
- (14) Strassner, J. E. Effect of pH on interfacial films and stability of crude oil–water emulsions. *J. Pet. Technol.* **1968**, *20*, 303–312.
- (15) Lucassen-Reynders, E. H.; et al. Dynamic surface studies as a tool to obtain equation-of-state data for soluble monolayers. In *Monolayers*; Goddard, E. D., Ed.; American Chemical Society (ACS): Washington, D.C., 1975; *Advances in Chemical Series*, Vol. 144, Chapter 21, pp 272–285.
- (16) Benjamins, J.; Cagna, A.; Lucassen-Reynders, E. H. Viscoelastic properties of triacylglycerol/water interfaces covered by proteins. *Colloids Surf., A* **1996**, *114*, 245–254.
- (17) Bouriat, P.; et al. Properties of a two-dimensional asphaltene network at the water/cyclohexane interface deduced from dynamic tensiometry. *Langmuir* **2004**, *20*, 7459–7464.
- (18) Fainerman, V. B.; Makievski, A. V.; Miller, R. The analysis of dynamic surface tension of sodium alkyl sulfate solutions, based on asymptotic equations of adsorption kinetic theory. *Colloid Surf., A* **1994**, *87*, 61–75.
- (19) C_b is found slightly lower for DAO, which suggests that they are not totally insoluble in *n*-heptane.
- (20) Baugé, F.; Langevin, D.; Lenormand, R. Dynamic surface properties of asphaltenes and resins at the oil/air interface. *J. Colloid Interface Sci.* **2001**, *239*, 501–508.
- (21) Janardhan, R.; Gedam, P. H.; Sampathkumaran, P. S. The effect of polymer molecular weight in the adsorption process. *J. Colloid Interface Sci.* **1990**, *140* (2), 391–400.
- (22) Kawaguchi, M. Sequential polymer adsorption: Competition and displacement process. *Adv. Colloid Interface Sci.* **1990**, *32* (1), 1–41.
- (23) Andreatta, G.; et al. Nanoaggregates and structure–function relations in asphaltenes. *Langmuir* **2005**, *21*, 1282–1289.
- (24) Groenzin, H.; Mullins, O. C. Asphaltene molecular size and weight by time-resolved fluorescence depolarization. *Asphaltenes, Heavy Oils and Petroleomics*; Springer: New York, 2007; pp 17–62.
- (25) Barré, L.; et al. Relation between nanoscale structure of asphaltene aggregates and their macroscopic solution properties. *Oil Gas Sci. Technol.* **2009**, *64*, 617–1628.
- (26) Freed, D. E.; et al. Molecular composition and dynamics of oils from diffusion measurements. *Asphaltenes, Heavy Oils and Petroleomics*; Springer: New York, 2007; pp 279–299.
- (27) Lobato, M. D.; et al. Optical characterization of asphaltenes at the air–water interface. *Langmuir* **2009**, *25*, 1377–1384.
- (28) Orbulescu, J.; Mullins, O. C.; Leblanc, R. M. Surface chemistry and spectroscopy of UG8 asphaltene Langmuir film, part 1. *Langmuir* **2010**, *26*, 15257–15264.